Orographic disturbances of surface winds over the shelf waters adjacent to South Georgia

[*Short title: Orographic disturbances of surface winds around South Georgia*]

J. Scott Hosking*, Daniel Bannister, Andrew Orr, John King, Emma Young and Tony Phillips

British Antarctic Survey, NERC, Cambridge, UK

For submission to *Atmospheric Science Letters*

Revised version: 25 June 2014

* Corresponding Author
J. Scott Hosking (jask@bas.ac.uk)
British Antarctic Survey
Madingley Road, High Cross
Cambridge, Cambridgeshire, CB3 0ET
TEL: 01223 221499

Abstract

This study seeks to quantify the influence of South Georgia's orography on regional surface winds. A typical case study characterised by large-scale westerly winds is analysed using a high-resolution setup (3.3 km) of the WRF regional model. The simulation produces significant fine-scale spatial variability which is in agreement with satellite derived winds. The model simulation indicates that these orography-driven wind disturbances are responsible for strong wind stress curl and enhanced heat flux over the shelf waters surrounding South Georgia. Such surface forcing is entirely absent from the reanalysis, highlighting the need to use high-resolution forcing in regional ocean model simulations.

1. Introduction

South Georgia is an extremely mountainous and narrow island located in the southern Atlantic Ocean (Figure 1a). With an approximate southeast-northwest orientation, it is roughly 170 km long and 2-40 km wide, contains 11 peaks exceeding 2000 m, and is separated from the surrounding deep ocean by shallow shelf waters of about 50-150 km width and mostly less than 300 m deep (Figure 1b). It lies within a region of strong mean westerly winds, which are variable on short time-scales due to storms caused by intense cyclonic activity. The focus of this article is the influence of South Georgia's orography on these winds and in the associated air-sea interaction.

Orographic induced disturbance of large-scale winds by islands can result in significant regional near-surface wind variations (Etling 1989, 1990; Smith et al, 1997), which in turn can generate variations in the dynamical and thermal coupling between the atmosphere and the ocean that are important for the mean state and variability of the oceanic circulation (e.g., Xie *et al.*, 2001; Chelton *et al.*, 2004; Dong and McWilliams, 2007; Pullen *et al.*, 2008; Couvelard *et al.*, 2012). Around South Georgia the shelf waters often show properties that are markedly different from the open ocean waters beyond (Brandon *et al.*, 2000; Meredith *et al.*, 2005), indicating that local processes are also important in dictating shelf water characteristics at this location. Despite the importance of these waters as one of the most biodiverse marine ecosystems on Earth (Hogg *et al.*, 2011), their response to atmospheric forcing at fine spatial scales has not been investigated.

Young *et al.* (2011, 2012, 2014) have studied the circulation of the South Georgia shelf and surrounding deeper ocean using a high-resolution ocean model driven by atmospheric forcing derived from reanalysis data. However, the coarse spatial resolution of reanalyses is not able to adequately represent the orography of South Georgia, nor is it able to explicitly resolve fine-scale wind features (e.g., Yuan, 2004; Risien and Chelton, 2008). To overcome this problem in other study areas, mesoscale atmospheric models with a horizontal resolution of a few kilometres have been used to dynamically downscale the reanalysis data in order to resolve the missing small-scale features generated by the orography. The more realistic atmospheric forcing thus generated can be used to force an ocean model (e.g., Dong and McWilliams, 2007; Couvelard *et al.*, 2012).

The objective of the present study is to quantify the impact of orographic forcing on the wind field over the shelf waters adjacent to South Georgia. We address this question by using the Weather Research and Forecasting (WRF) atmospheric model at high spatial resolution to dynamically downscale reanalysis data for the South Georgia region. After characterising the improvement by comparison with scatterometer measurements of the surface wind field, output from the WRF model is used to determine the associated forcing of the underlying ocean.

2. Methods, model and data

A single case study on 13 September 1999 of westerly flow with a 10 m wind speed of approximately 13 – 14 m s^{-1} is selected. The pertinence of this case study can be gauged by comparison with the climatological wind rose for 10 m winds at King Edward Point as shown in Figure 2, produced from ERA Interim reanalysis data which has a N128 (0.7° × 0.7°, ~45 km × ~80 km near South Georgia) spatial resolution (Dee *et al.*, 2011). This shows that it is representative of atmospheric conditions around South Georgia, which are typified by primarily westerly winds with speeds in the range of 7.5 – 15 m s^{-1}.

The WRF model is an atmosphere-only, limited-area, non-hydrostatic, mesoscale modelling system (http://www.wrf-model.org). Here we utilise WRF version 3.4.1 (Skamarock et al, 2008). The configuration of the three nested domains (one-way interaction) used in our study is illustrated in Figure 1a. The outer domain has 75 × 45 grid points at a horizontal grid-spacing of 30 km, covering a relatively large ocean area in order to better resolve the

prevailing westerly winds of the Southern Ocean, and particularly the representation of small mesocyclones (scales of a few hundred kilometers) which are also inadequately represented by reanalysis (Condron *et al.*, 2006). The intermediate domain has 115 × 91 grid points and a horizontal grid-spacing of 10 km. The innermost domain has 151 × 151 grid points at a horizontal grid-spacing of 3.3 km, covering South Georgia and the surrounding shelf sea (illustrated by the zoomed in map in Fig 1b). All domains have a total of 70 vertical levels and a model top at 10 hPa. ERA-Interim was used to initialize the surface and lateral boundary conditions for the outer domain and to update them every 6 hours as the model is integrated forward. The WRF run started at 0000 UTC 12 September 1999 and ended at 1800 UTC 13 September 1999. Only model output from the innermost 3.3 km resolution domain is discussed.

To improve the representation of resolved orographic effects, the model topography was generated using the 90 m resolution Shuttle Radar Topography Mission (Jarvis *et al.*, 2008) dataset (the standard topography in WRF is derived from a dataset which has a resolution of approximately 1 km). Similarly, to improve the representation of the land surface, the model land use classification was generated from 90 m resolution Landsat satellite data which correctly classified South Georgia's higher elevations as 'permanent snow cover' (the standard land-use field in WRF erroneously classified South Georgia as entirely 'bare rock').

Preliminary sensitivity experiments testing various physics options for the WRF model were conducted for a range of contrasting meteorological conditions, with the model output being compared against measurements of pressure, temperature, wind speed and direction at King Edward Point, South Georgia (see Figure 1b for location). Based on this the physics choices selected include the New Goddard scheme for longwave and shortwave radiation (Chou and Suarez, 1999), the Mellor-Yamada-Nakanishi-Niino Level 2.5 planetary boundary layer scheme (Nakanishi and Niino, 2004), the unified Noah land-surface model (Chen and Dudhia, 2001), and the Kain-Fritsch cumulus scheme (Kain and Fritsch, 1993). Due to the steeply sloping terrain and high horizontal and vertical resolution, an adaptive time step (rather than fixed) was required in order to rectify computational instability.

The WRF model results are compared to near-surface (10 m) wind fields obtained from the Quick Scatterometer (QuikSCAT), which were obtained from the Jet Propulsion Laboratory website (ftp://podaac-ftp.jpl.nasa.gov/allData/quikscat/L3/jpl/v2/hdf/). This dataset has a

spatial resolution of 0.25° (~25 km), but is unable to provide observations over land and so consequently winds over South Georgia and its nearshore regions are excluded. QuikSCAT wind data are accurate to within 1-2 m s^{-1} in speed and 20-30° in direction (e.g., Ebuchi *et al.*, 2002; Sousa *et al.*, 2013).

WRF is subsequently used to determine the associated patterns of surface wind stress curl and surface heat flux, which both exert strong controls on ocean circulation and water column structure. To this end the surface wind stress is computed from WRF 10 m winds using the formulation of Large and Pond (1982) to calculate the drag coefficient.

3. Results

Figure 3 shows the observed (a) and simulated 10 m (b) wind field over the shelf waters adjacent to South Georgia. It should be noted that orography driven disturbances are entirely absent from ERA-Interim wind field (c). This is unsurprising given that South Georgia is not resolved by ERA-Interim, i.e., ERA-Interim treats all the grid cells containing South Georgia as ocean and therefore completely fails to represent its orography and land-sea distribution.

Assuming wind speed U ~ 14 m s^{-1}, mountain height h ~ 2000 m, buoyancy frequency N ~ 0.01 s^{-1}, mountain half-width D ~ 20 km, and Coriolis parameter f ~ -1.2×10^{-4} s^{-1}) then the non-dimensional mountain height ($\hat{h} = Nh/U$) and the Rossby number ($\mathrm{Ro} = U/|f|D$) are $\hat{h} \sim 1.4$ and Ro ~ 5.8, respectively. This suggests that the flow response generated by the orography will be characterised by non-linear behaviour (i.e., $\hat{h} > 1$) where the effects of rotation are important (i.e., Ro < 10), as reviewed by Orr *et al.* (2005, 2008). Figure 3a shows a number of features in the observed wind field which are consistent with this, most notably deceleration of the incident flow, flow splitting around the island (diverting more to the right when looking downwind), a wake of relatively weak winds of approximately 10 - 11 m s^{-1} extending many hundreds of kilometres downstream of the island, and the formation of wind jets of up to 18 m s^{-1} either side of the wake (with wind speeds greater on the right-hand side than the left-hand side). Comparison with Figure 3b shows that the WRF simulation agrees qualitatively well with the QuikSCAT winds, although in the model the wind jets are 1 – 2 m s^{-1} too weak and the modelled wake region does not extend far enough downstream or close enough to South Georgia.

The features described above are readily identifiable in fields of wind stress curl and sensible and latent heat fluxes from WRF, as shown in Figure 4 (including over the near-shore waters where QuikSCAT data are absent). Here we primarily focus on wind-induced forcing over the shelf sea waters, i.e., the area confined within the 300 m bathymetry depth contour. The high-speed (17-18 ms^{-1}) wind jet off the southern tip of the island, as seen in Figure 3b around 35.5°W and 55.2°S, is associated with a large upward (positive) sensible heat flux exceeding 50 W m^{-2}, while surface forcing from wind stress curl and latent heat fluxes are less marked at around 1.6×10^{-5} Nm^{-3} and 70 W m^{-2}, respectively. In the wake of weak winds there are regions of both negative and positive wind stress curl with magnitudes in excess of 4×10^{-5} Nm^{-3}. This coincides with relatively weak downward sensible heat fluxes of between -30 and 0 W m^{-2}, and upward latent heat flux exceeding 100 W m^{-2} (i.e., the net heat flux is upward). Comparison with ERA-Interim (not shown) indicates that magnitudes of wind stress curl are typically two orders of magnitude greater than the corresponding variables in the reanalysis. Furthermore, the WRF sensible heat fluxes are around one order of magnitude larger, while latent heat fluxes are around twice those derived by ERA-Interim.

4. Summary and discussion

This study shows that fine-scale structure in winds, forced by South Georgia's steep orography, contribute to the generation of important surface forcing of the surrounding shelf seas, e.g., wind stress curl of the order 10^{-5} N m^{-3} is the same order of magnitude as that observed over the Irminger Sea forced by the Greenland tip jet (Pickart et al., 2003). Wind effects such as these are consistent with non-linear (i.e., $\hat{h} > 1$) flow regimes where the effects of rotation are important (i.e., Ro < 10). For the range of 10 m wind speeds suggested to typify South Georgia (7.5 – 15 m s^{-1}), the associated values of $\hat{h}$ and Ro would lie in the range 1.3 to 2.7 and 3 to 6, respectively, indicating that South Georgia is frequently associated with these effects. Such fine-scale wind effects and their subsequent surface forcing were entirely missing from the reanalysis, i.e., the corresponding values of wind stress curl in the reanalysis were two orders of magnitude less than that simulated by WRF (not shown).

Together the high values of wind stress curl and air-sea heat flux would force complex localised ocean circulation features, such as wind-driven gyres or downwelling, which would then drive changes in sea-surface temperature. Additionally, localised sea-surface temperatures would also be affected by, e.g., changes in precipitation and incident solar radiation due to the influence of South Georgia on clouds. However, as we are using an atmosphere-only (uncoupled) model, we are unable to account for how these changes to sea-surface temperature would feed back on the atmosphere (Businger and Shaw, 1984; Caldeira and Tomé, 2013). Addressing such feedbacks would require a coupled atmosphere-ocean regional model, which is an area for further work. Nevertheless, we assert that any such feedback effects would be of secondary significance relative to the gross modification of the regional wind field by the orography, and the impact this would have on the ocean current system.

Understanding of the influence of complex wind-driven oceanic circulation features is vital for insight into local marine ecosystem dynamics. The waters surrounding South Georgia are amongst the most biologically productive in the Southern Ocean, supporting vast local colonies of higher predators, including penguins and fur seals, as well as significant international fisheries (Atkinson *et al.*, 2001; Kock *et al.*, 2011). Previous ocean modelling work using atmospheric forcing derived from reanalysis demonstrated that South Georgia's marine ecosystem dynamics are strongly influenced by variability in the underlying oceanography (Young *et al.*, 2012, 2014). However, our study suggests that using reanalysis data for the atmospheric forcing would have resulted in unrealistically weak spatial and temporal variability in the local oceanography due to the failure to capture important wind-driven complex circulation features. This study thus highlights the need to use high spatial resolution wind forcing in a regional ocean model.

Acknowledgements

The case study examined in this article was also a focus of the Jet Propulsion Laboratory 'Photojournal' (http://photojournal.jpl.nasa.gov/catalog/PIA02457). Daniel Bannister was supported by a PhD studentship funded by the UK Natural Environment Research Council.

References

Atkinson A, Whitehouse MJ, Priddle J, Cripps GC, Ward P, Brandon MA. 2001. South Georgia, Antarctica: a productive, coldwater pelagic ecosystem. Marine Ecology Progress Series 216: 279–308.

Brandon MA, Murphy EJ, Trathan PN, Bone DG. 2000. Physical oceanographic conditions to the northwest of the sub-Antarctic Island of South Georgia. *Journal of Geophysical Research* **105**: 23983-23996.

Businger JA, Shaw WJ. 1984. The response of the marine boundary layer to mesoscale variations in sea-surface temperature. *Dyn. Atmos. Ocean*. 8, 267–281.

Caldeira RM, Tomé R. 2013. Wake Response to an Ocean-Feedback Mechanism: Madeira Island Case Study. *Bound. Layer Meteorol*. 148, 419–436.

Chelton DB, Schlax MG, Freilich MH, Milliff RF. 2004. Satellite measurements reveal persistent small-scale features in ocean winds. *Science* **303:** 978-983.

Chen F, Dudhia J. 2001. Coupling an advanced land surface-hydrology model with the Penn State-NCAR MM5 modelling system. Part I: Model implementation and sensitivity. *Monthly Weather Review* **129**: 569-585.

Chou M-D, Suarez MJ. 1999. A solar radiation parameterization for atmospheric studies. Technical Report Series on Global Modeling and Data Assimilation, MJ Suarez (Ed.), NASA/TM-1999-104606, Vol. 15, Goddard Space Flight Center, Greenbelt, MD, 42 pp.

Condron A, Bigg GR, Renfrew IA. 2006. Polar mesoscale cyclones in the northeast Atlantic: Comparing climatologies from ERA-40 and satellite imagery. *Monthly Weather Review* **134**: 1518-1533.

Couvelard X, Caldeira RMA, Araújo IB, Tomé R. 2012. Wind mediated vorticity-generated and eddy-confinement, leeward of the Madeira Island: 2008 numerical case study. *Dynamics of Atmospheres and Oceans* **58**: 128-149.

Dee DP, Uppala SM, Simmons AJ, Berrisford P, Poli P, Kobayashi S, Andrae U, Balmaseda MA, Balsamo G, Bauer P, Bechtold P, Beljaars ACM, van de Berg L, Bidlot J, Bormann N, Delsol C, Dragani R, Fuentes M, Geer AJ, Haimberfer L, Healy SB, Hersbach H, Hólm EV, Isaksen L, Kållberg P, Köhler M, Matricard M, McNally AP, Monge-Sanz BM, Morcrette JJ, Park BK Peubey C, de Rosnay P, Tavolato C, Thépaut JN, Vitart F. 2011. The ERA-Interim reanalysis: configuration and performance of the data assimilation system. *Quarterly Journal of the Royal Meteorological Society* **137**: 553 - 597.

Dong C, McWilliams JC. 2007. A numerical study of island wakes in the Southern California Bight. *Continental Shelf Research* **27**: 1233-1248.

Ebuchi N, Graber HC, Caruso MJ. 2002. Evaluation of wind vectors observed by QuikSCAT/SeaWinds using ocean buoy data. *Journal of Atmospheric and Oceanic Technology* **19**: 2049-2062.

Etling D. 1989. On atmospheric vortex streets in the wake of large islands. *Meteorology and Atmospheric Physics*, 41(3), 157–164.

Etling D. 1990. Mesoscale vortex shedding from large islands: A comparison with laboratory experiments of rotating stratified flows. *Meteorology and Atmospheric Physics*, 43(1-4), 145–151. Hogg OT, Barnes DKA, Griffiths HJ. 2011. Highly diverse, poorly studied and uniquely threatened by climate change: An assessment of marine biodiversity on South Georgia's continental shelf. *PLoS ONE* **6**: e19795. doi: 10.1371/journal.pone.0019795.

Jarvis A, Reuter HI, Nelson A, Guevara E. 2008. Hole-filled SRTM for the globe Version 4. Available from the CGIAR-CSI SRTM 90 m Database (http://srtm.csi.cgiar.org).

Kain JS, Fritsch JM. 1993. Convective parameterization for mesoscale models: The Kain-Fritsch scheme. *The Representation of Cumulus Convection in Numerical Models, Meteorological Monographs* **46**: 165-170.

Kock K-H, Reid K, Croxall J, Nicol S. 2007. Fisheries in the Southern Ocean: an ecosystem approach. Philosophical Transactions of the Royal Society of London. Series B 362(1488): 2333–2349, DOI: 10.1098/rstb.2006.1954.

Large WG, Pond S. 1982. Sensible and latent heat flux measurements over the ocean. *Journal of Physical Oceanography* **12**: 464-482.

Meredith MP, Brandon MA, Murphy EJ, Trathan PN, Thorpe SE, Bone DG, Chernyshkov PP, Sushin VA. 2005. Variability in hydrographic conditions to the east and northwest of South Georgia, 1996–2001. *Journal of Marine Systems* **53**: 143-167.

Nakanishi M, Niino H. 2004. An Improved Mellor–Yamada Level-3 Model with Condensation Physics: Its Design and Verification. *Boundary-Layer Meteorology*, 112(1), 1–31

Orr A, Hanna E, Hunt JCR, Cappelen J, Steffen K, Stephens AG. 2005. Characteristics of stable flows over Greenland. *Pure and Applied Geophysics* **162**: 1747-1778.

Orr A, Marshall GJ, Hunt JCR, Sommeria J, Wang C-G, van Lipzig NPM, Cresswell D, King JC. Characteristics of summer airflow over the Antarctic Peninsula in response to recent strengthening of westerly circumpolar winds. *Journal of the Atmospheric Sciences* **65**: 1396-1413.

Pickart RS, Spall MA, Ribergaard MH, Moore GWK, Milliff RF. 2003. Deep convection in the Irminger Sea forced by the Greenland tip jet. *Nature* **424**: 152-156.

Pullen J, Doyle JD, May P, Chavanne C, Flament P, Arnone RA. 2008. Monsoon surges trigger oceanic eddy formulation and propagation in the lee of the Philippine Islands. *Geophysical Research Letters* **35**: L07604, DOI: 10.1029/2007GL033109.

Risien CM, Chelton DB. 2008. A global climatology of surface wind and wind stress fields from eight years of QuikSCAT data. *Journal of Physical Oceanography* **38**: 2379-2413.

Skamarock WC, Klemp JB, Dudhia J, Gill DO, Barker M, Duda KG, Powers JG. 2008. A description of the Advanced Research WRF Version 3 (pp. 1–113).

Smith RB, Gleason AC, Gluhosky PA, Grubišić V. 1997. The Wake of St. Vincent. *Journal of the Atmospheric Sciences*, 54(5), 606–623

Sousa MC, Alvarez I, Vaz N, Gomez-Gesteira M, Dias JM. 2013. Assessment of wind pattern accuracy from the QuikSCAT satellite and the WRF model along the Galician coast (northwest Iberian Peninsula). *Monthly Weather Review* **141**: 742-753.

Xie S-P, Liu WT, Liu Q, Nonaka M. 2001. Far-reaching effects of the Hawaiian Islands on the Pacific Ocean atmosphere. *Science* **292**: 2057-2060.

Young EF, Meredith MP, Murphy EJ, Carvalho GR. 2011. High resolution modelling of the shelf and open ocean adjacent to South Georgia, Southern Ocean. *Deep-Sea Research II* **58**: 1540-1552.

Young EF, Rock J, Meredith MP, Belchier M, Murphy EJ, Carvalho GR. 2012. Physical and behavioural influences on larval fish retention: contrasting patterns in two Antarctic fishes. *Marine Ecology Progress Series* **465**: 201-204.

Young EF, Thorpe, SE, Banglawala, N., Murphy, EJ. 2014. Variability in transport pathways on and around the South Georgia shelf, Southern Ocean: Implications for recruitment and retention. *Journal of Geophysical Research: Oceans* **119**(1):: DOI: 10.1002/2013JC009348

Yuan X. 2004. High-wind-speed evaluation in the Southern Ocean. *Journal of Geophysical Research* **109**: D13101 DOI: 10.1029/2003JD004179.

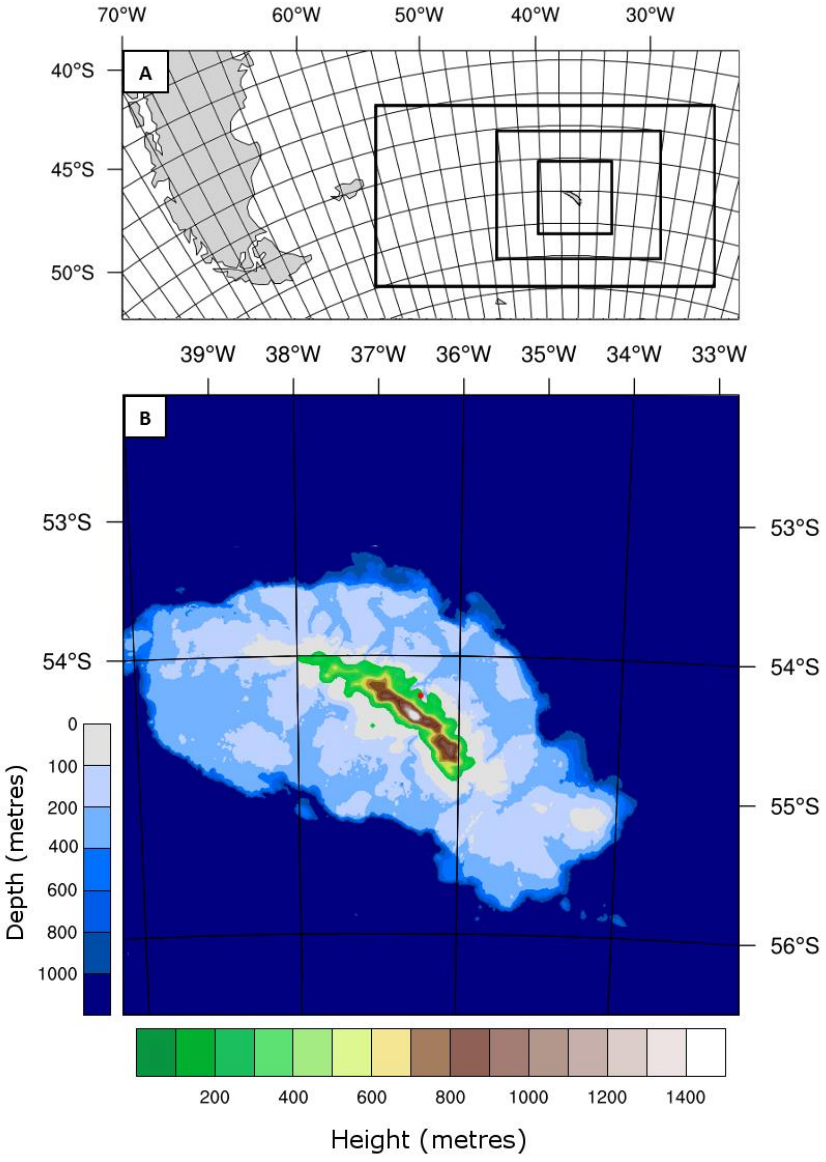

Figure 1: Regional maps to show the nested domain setup used for the South Georgia WRF model simulation. Panel (a) illustrates the lateral boundaries for the 30 km outer domain, 10 km intermediate domain, and the 3.3 km inner domain (black line boxes). A zoomed in map of the innermost domain is illustrated in panel (b), along with the bathymetry of the ocean shelf (blue shading), the island's orographic elevation at 3.3 km resolution (green-brown shading), and the location of King Edward Point (filled red circle)

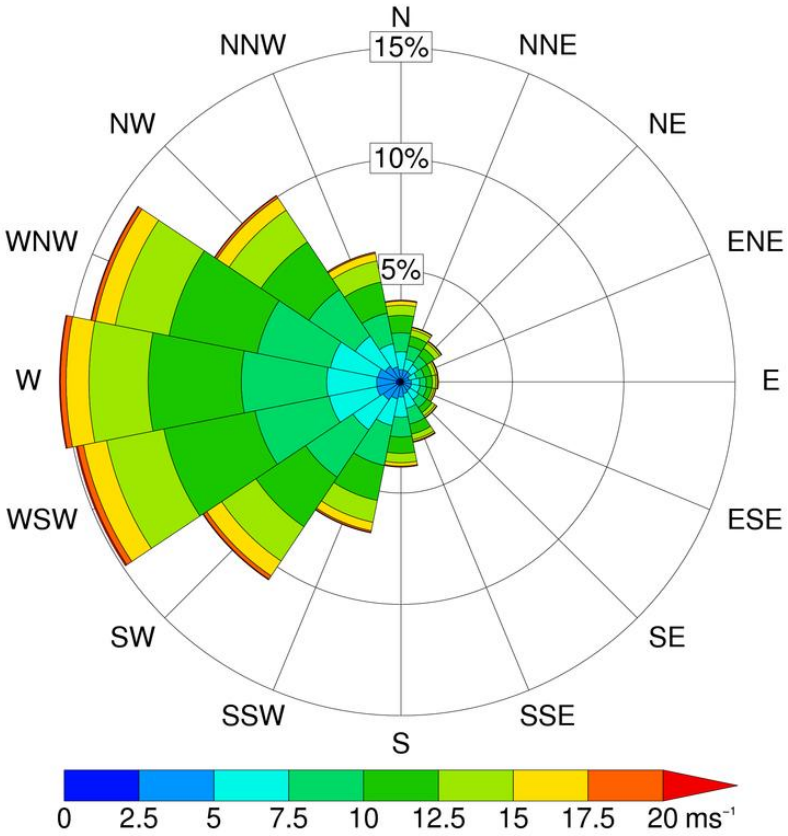

Figure 2: Climatological wind rose to illustrate the direction (°), frequency (%) and speed (m s^{-1}) of large-scale near-surface winds over the period 1979-2012. Data are interpolated from 6-hourly ERA-Interim reanalysis 10 m wind fields at King Edward Point, South Georgia (location indicated in Fig. 1b).

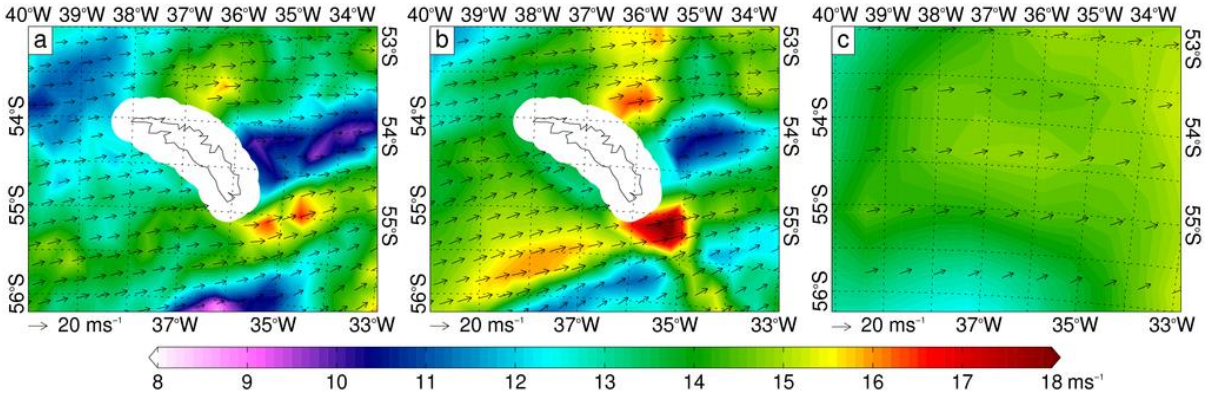

Figure 3: Comparison between observed, modelled and reanalysis 10 m winds (m s^{-1}) over the shelf waters adjacent to South Georgia for a case study on 13 September 1999 typical of the large-scale flow for the region. The panels show a) observations from QuikSCAT satellite mission at ~0900 UTC, b) WRF modelled 3.3 km resolution (re-sampled to the 'QuikSCAT' grid for fair comparison) at 0900 UTC, and c) ERA-Interim reanalysis at 1200 UTC. In panel (a) the 'blank' area indicates where the QuikSCAT wind data are unavailable, with the South Georgia coastline included for illustrative purposes. This is repeated in panel (b) for comparative purposes. As shown in panel (c), there is no representation of South Georgia within ERA-Interim reanalysis data.

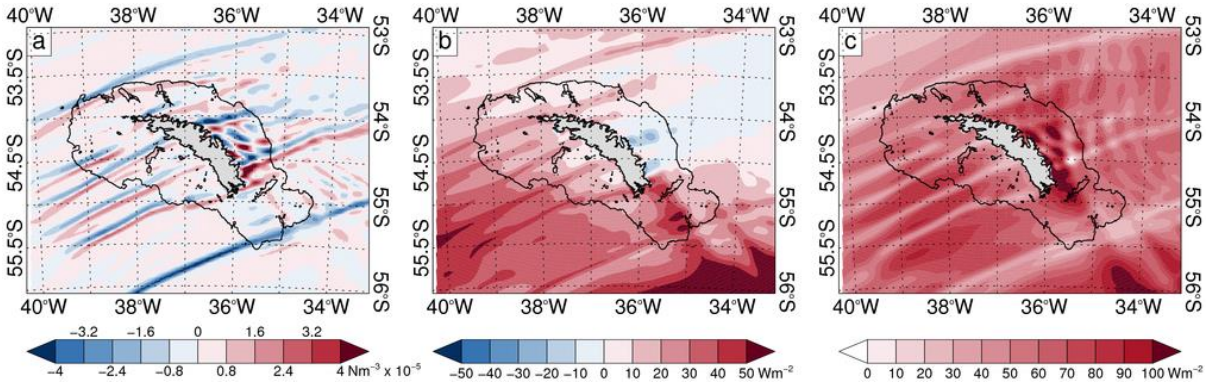

Figure 4: WRF modelled 3.3 km resolution surface forcing at 0900 UTC 13 September 1999 for a) wind stress curl (N $m^{-3} \times 10^{-5}$), b) sensible heat flux (W m^{-2}), and c) latent heat flux (W m^{-2}). Positive sensible and latent heat fluxes are upward. To highlight the sea shelf region, the 300 m bathymetry depth contour is included (black line).